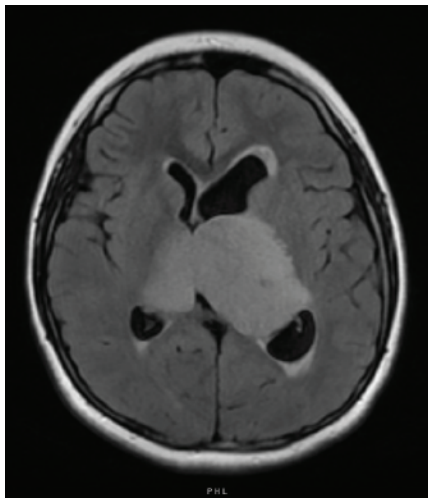
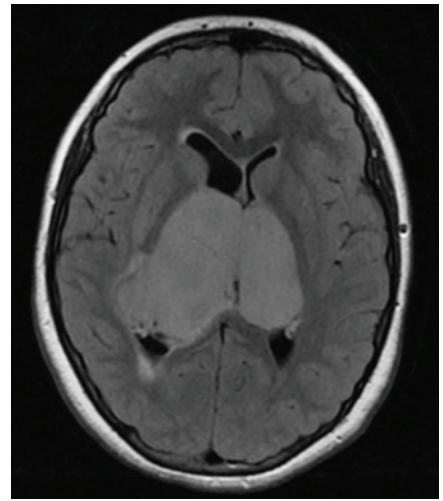


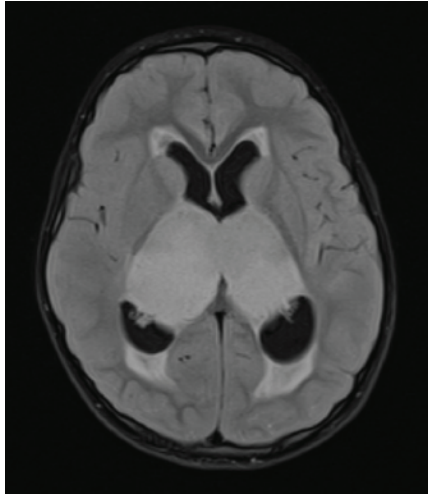
patient #1
11 y/o boy
anaplastic astrocytoma
EGFR ex20 indel
histone H3 wildtype



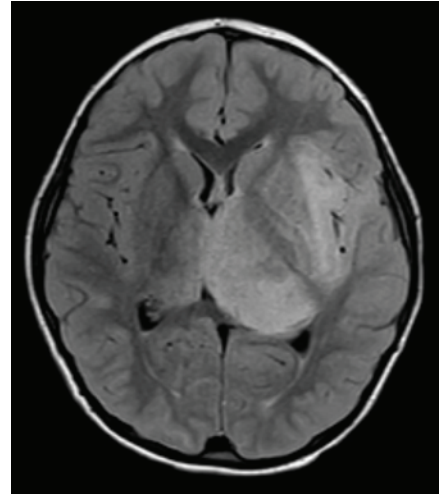
patient #3
11 y/o girl
anaplastic astrocytoma
EGFR ex20 indel
histone H3 wildtype



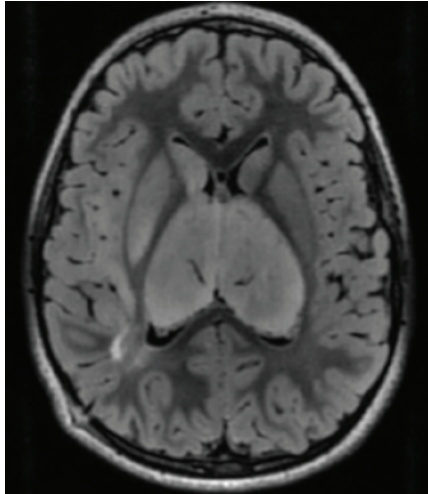
patient #5
3 y/o boy
diffuse astrocytoma
EGFR ex20 indel
histone H3 wildtype



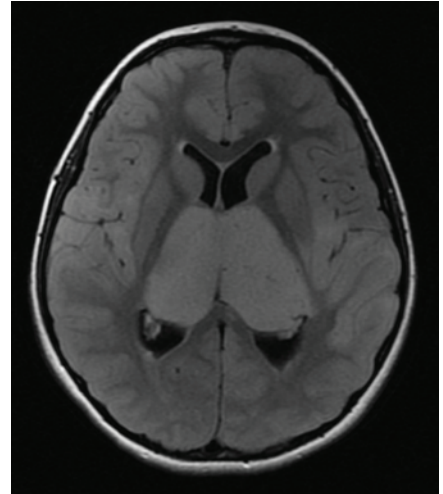
patient #8
6 y/o boy
diffuse astrocytoma
EGFR ex20 indel
histone H3 wildtype



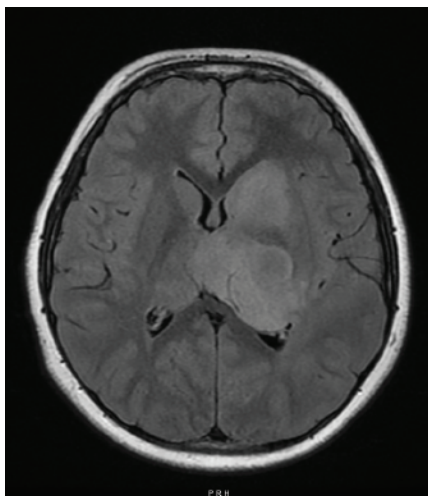
patient #10
5 y/o boy
anaplastic astrocytoma
EGFR p.A289T
histone H3 wildtype



patient #11
9 y/o girl
diffuse astrocytoma
EGFR p.A289V
HIST1H3B p.K27M

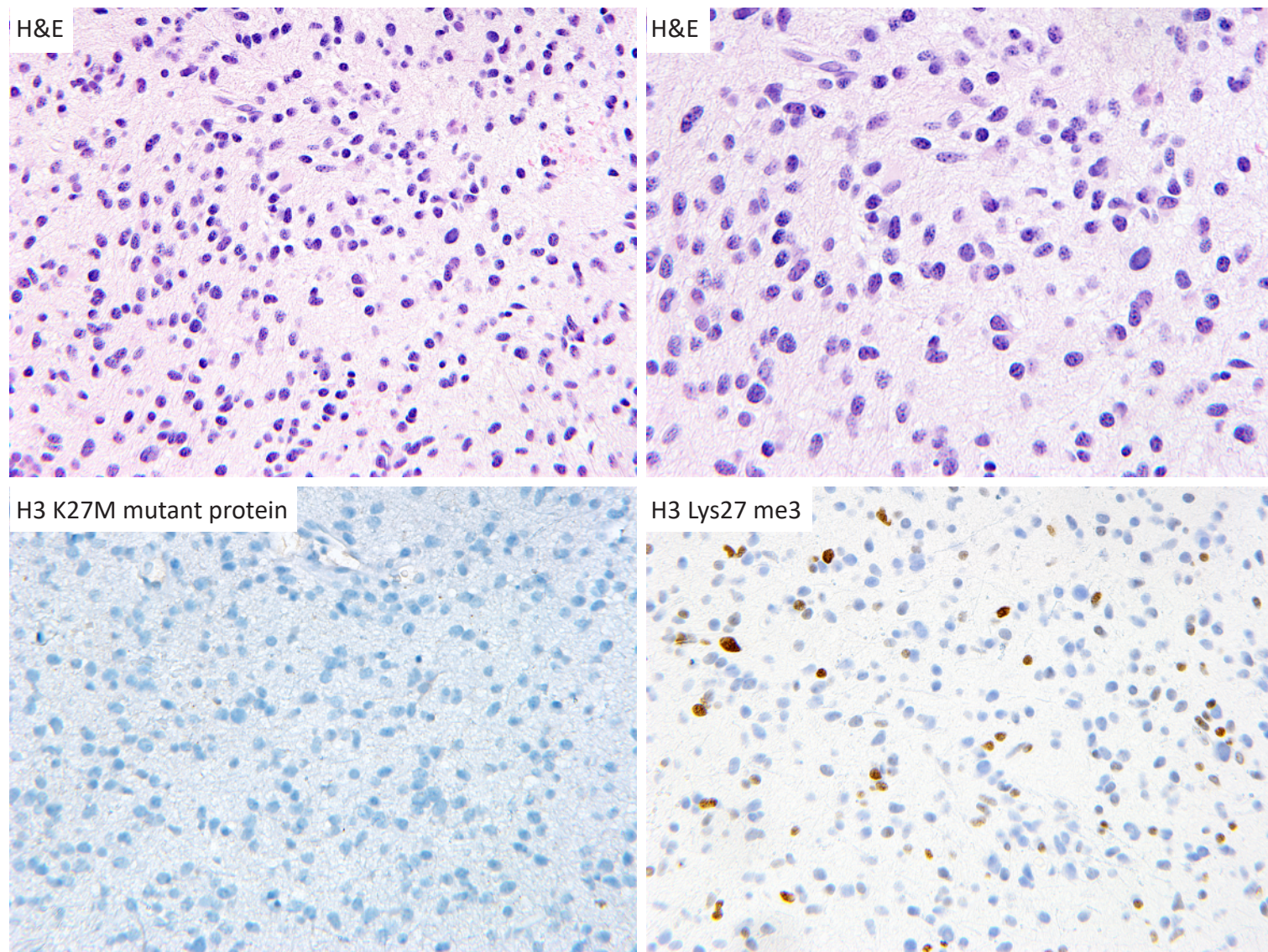


patient #13
9 y/o boy
anaplastic astrocytoma
EGFR wildtype
histone H3 wildtype



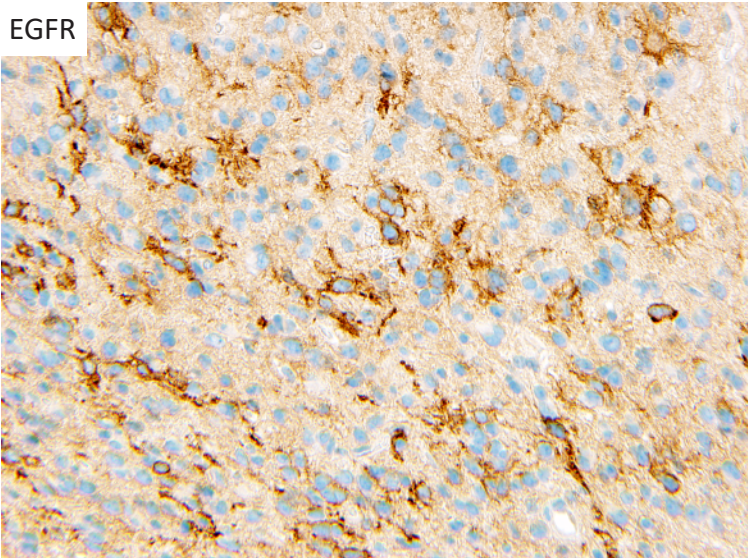
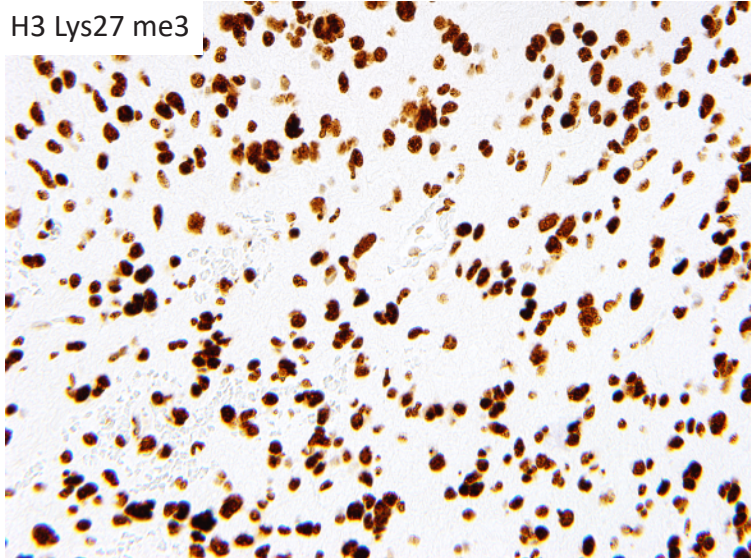
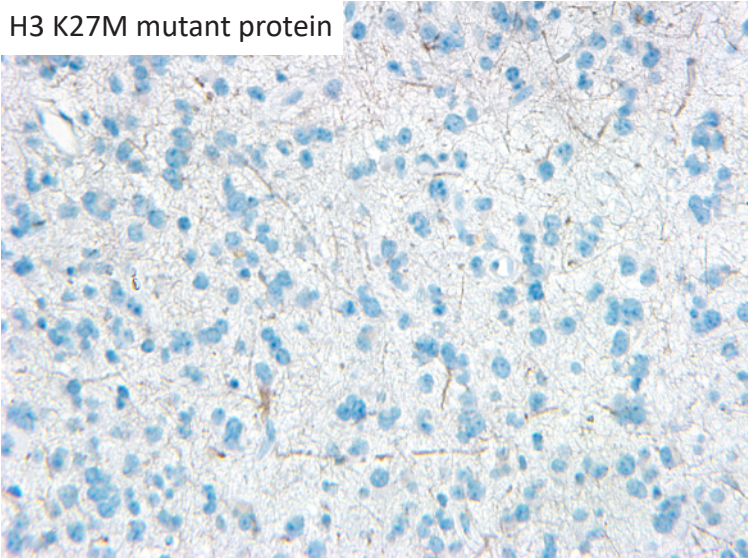
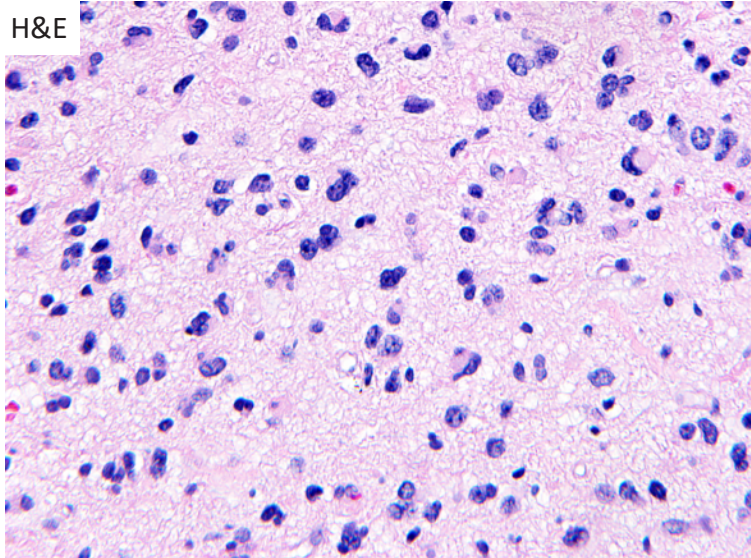
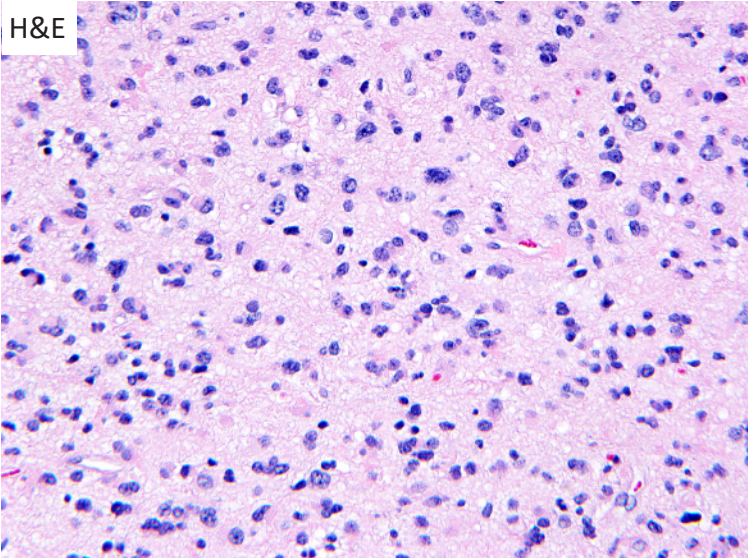
Supplementary Figure 1. Brain imaging from representative children with bithalamic diffuse gliomas. Axial T2-weighted fluid-attenuated inversion recovery images are shown.

patient #1, 11 y/o boy, anaplastic astrocytoma, EGFR ex20 indel, histone H3 wildtype

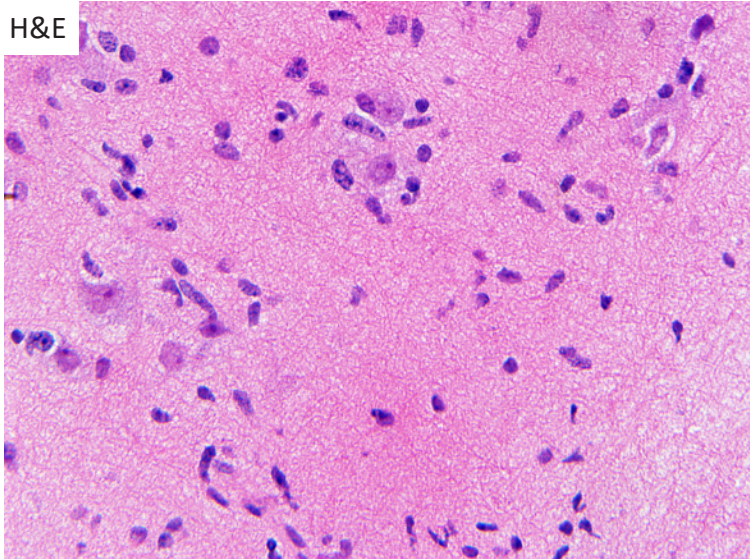
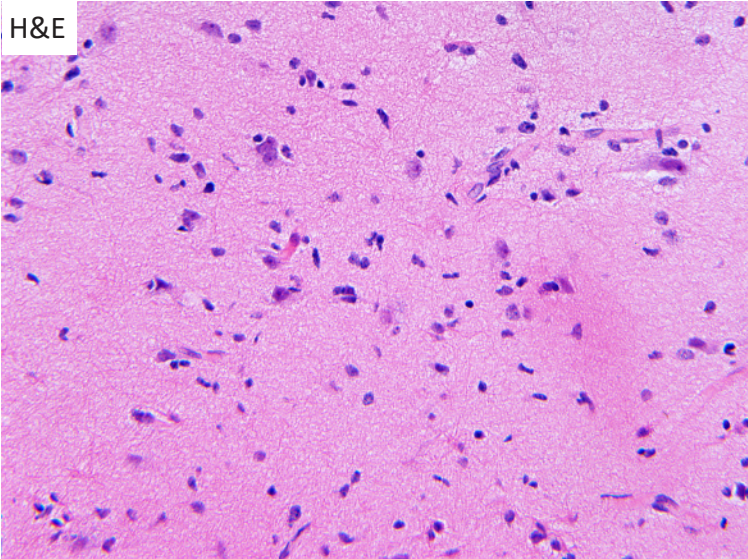


Supplementary Figure 2. Histologic features of representative bithalamic diffuse gliomas.

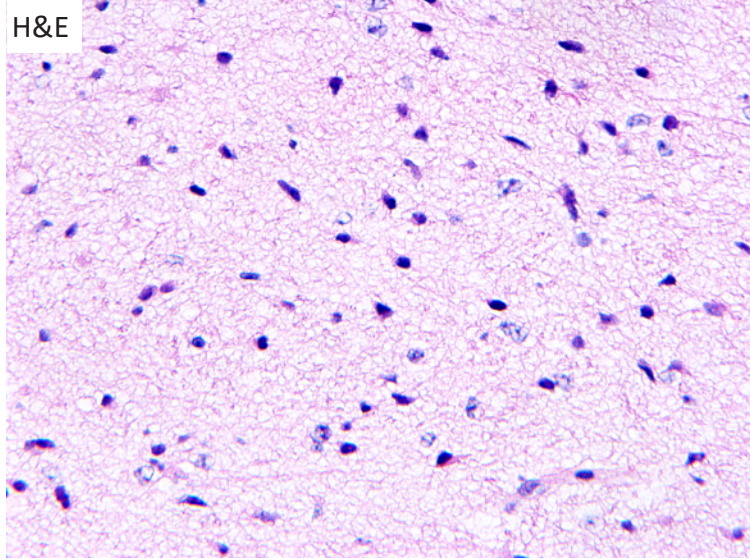
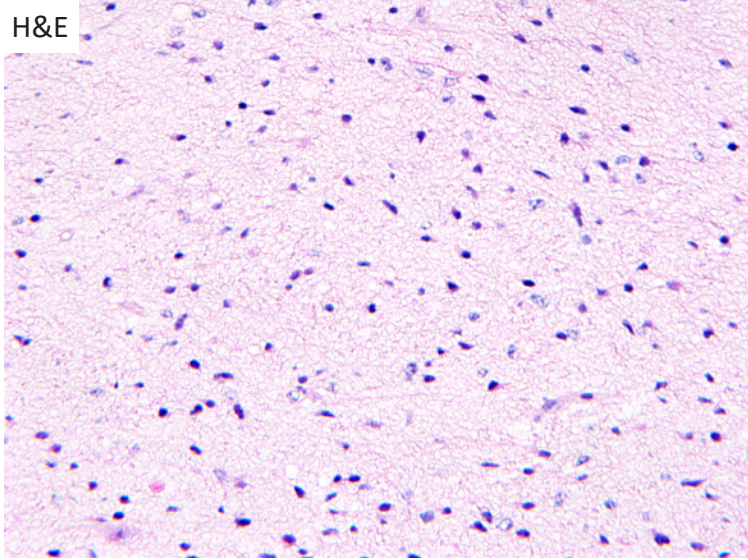
patient #3, 11 y/o girl, anaplastic astrocytoma, EGFR ex20 indel, histone H3 wildtype



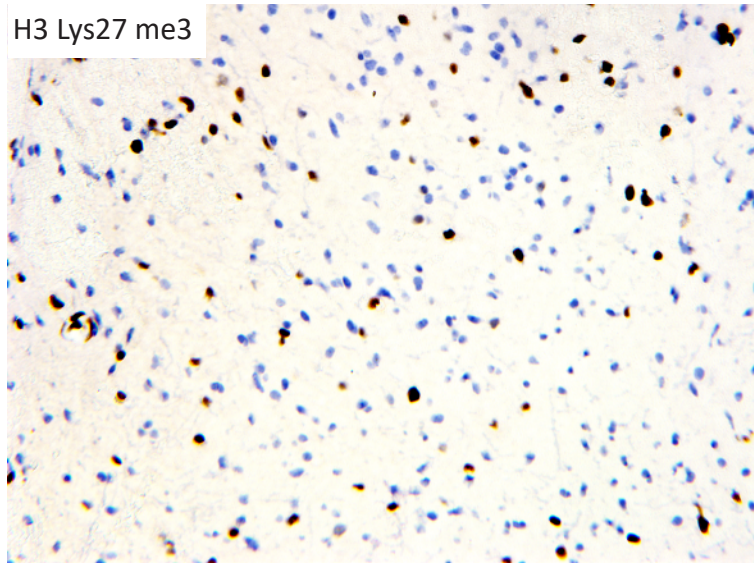
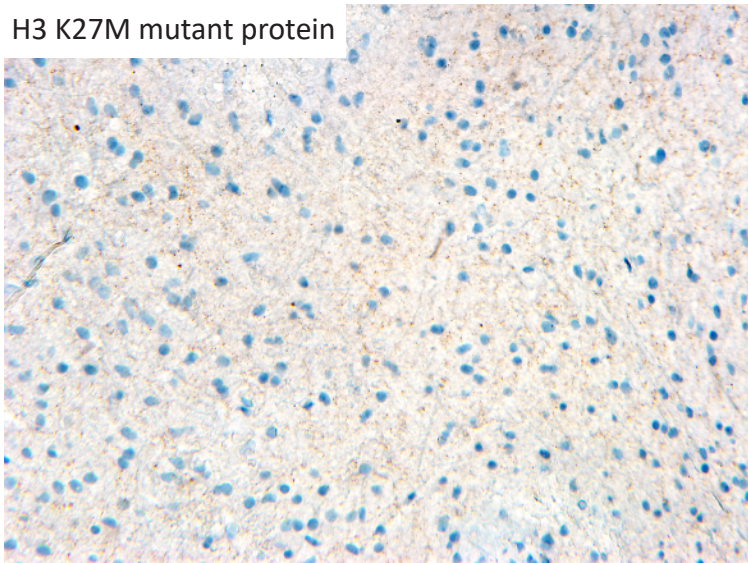
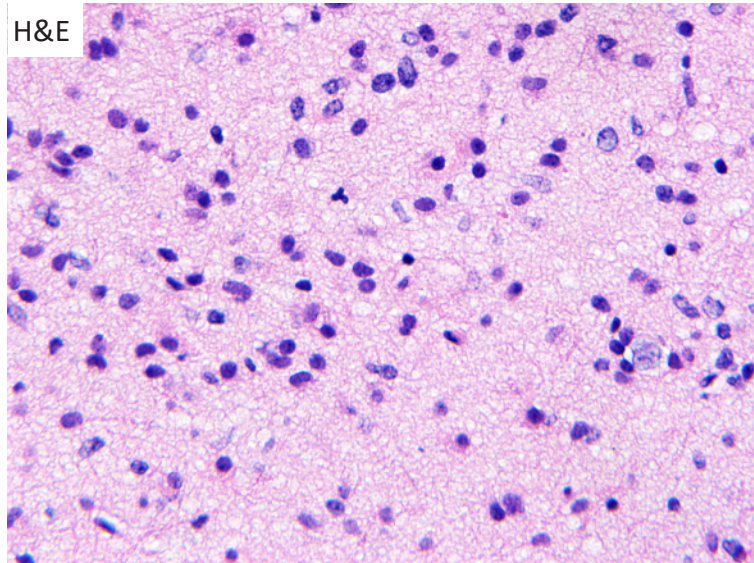
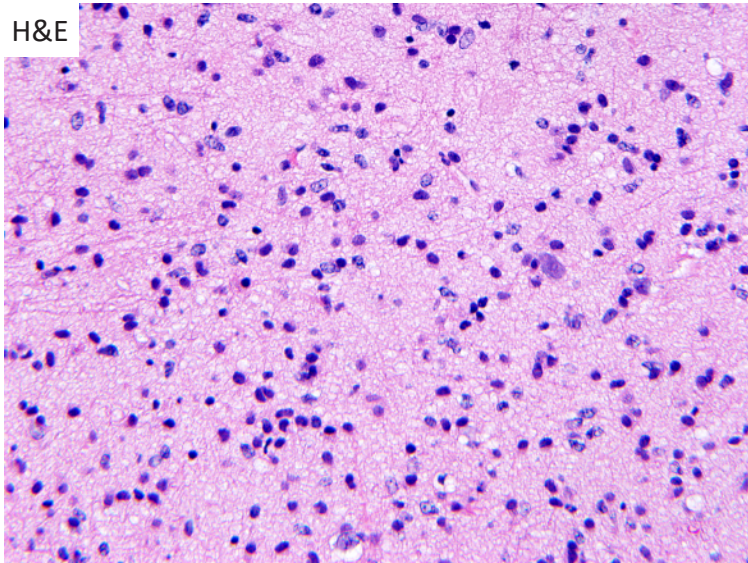
patient #5, 3 y/o boy, diffuse astrocytoma, EGFR ex20 indel, histone H3 wildtype



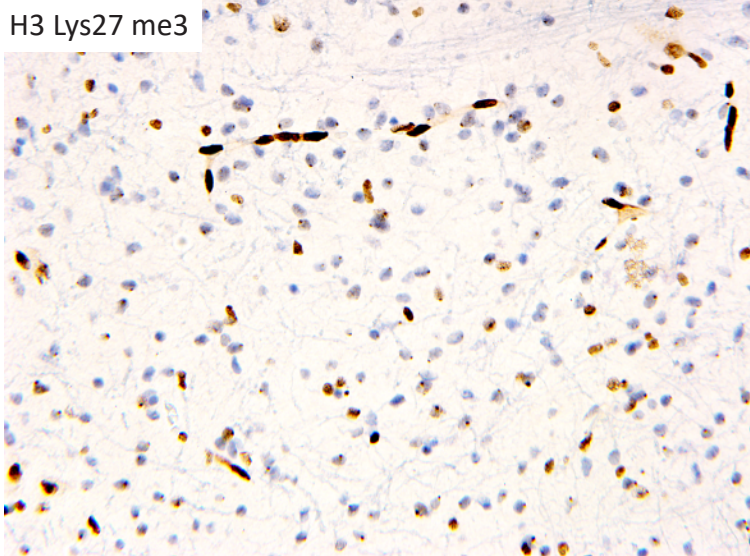
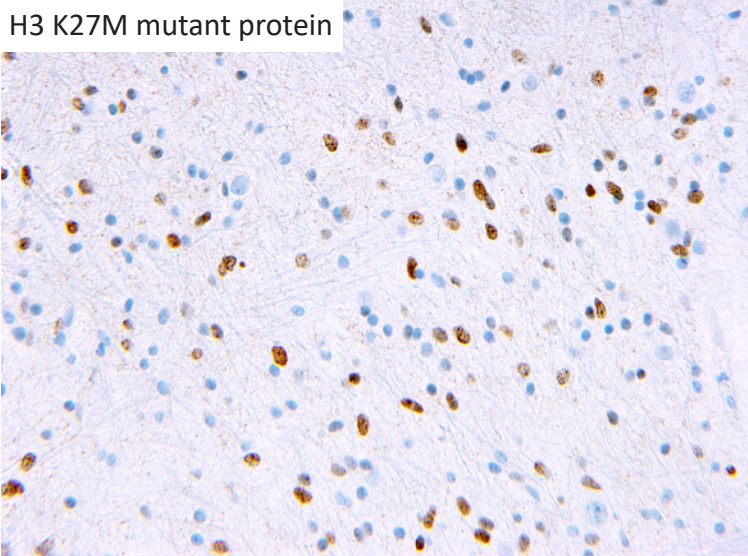
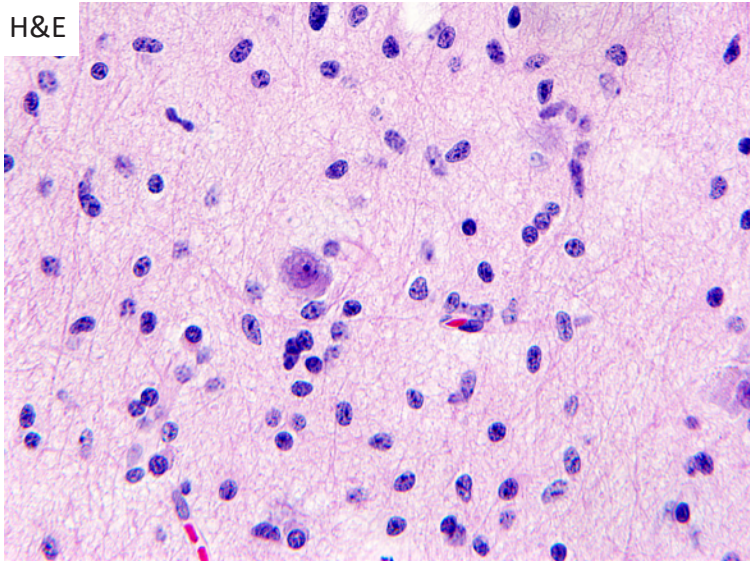
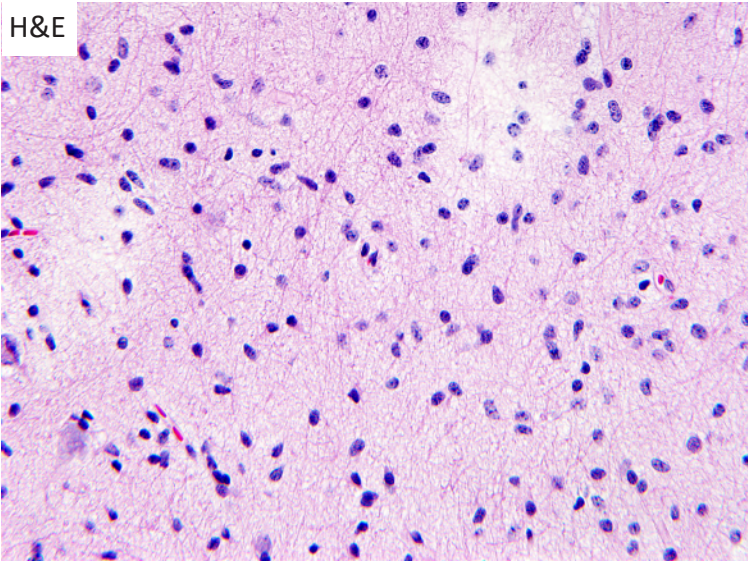
patient #8, 6 y/o boy, diffuse astrocytoma, EGFR ex20 indel, histone H3 wildtype



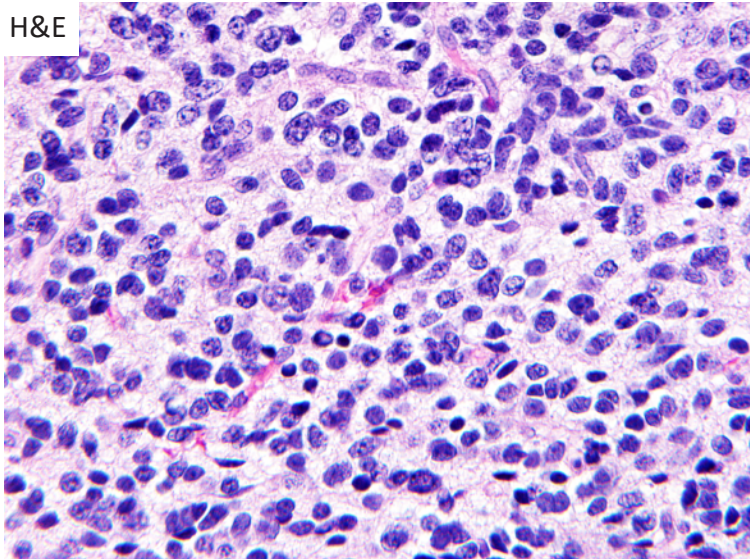
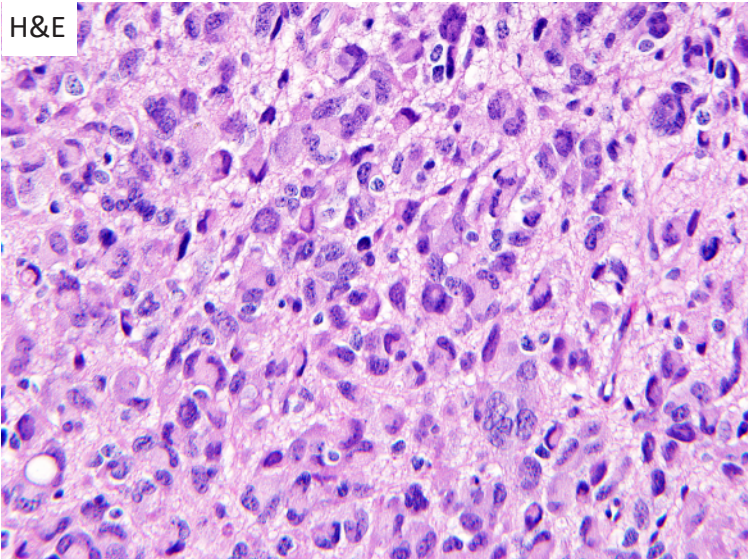
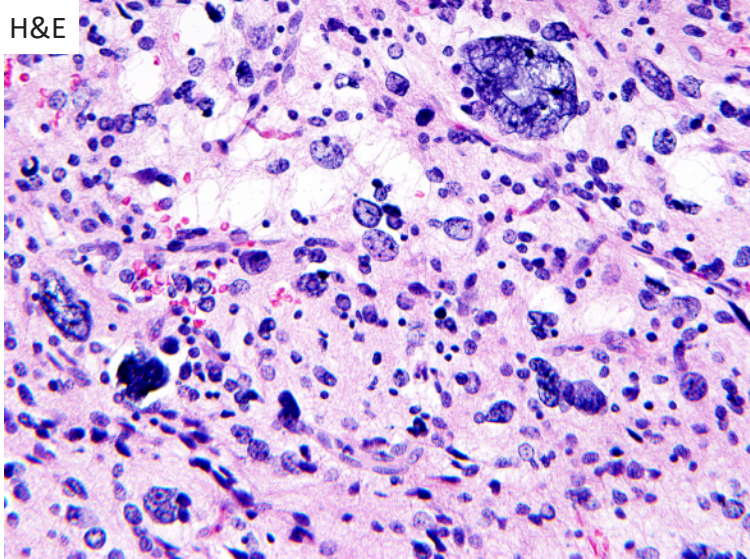
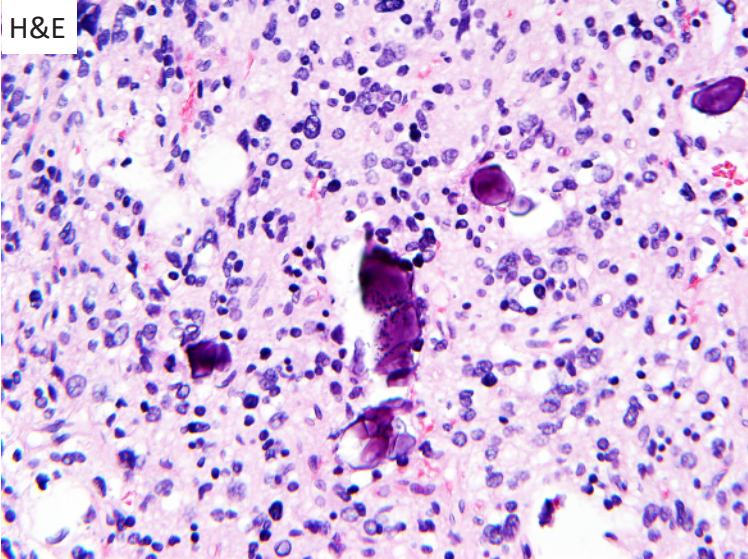
patient #10, 5 y/o boy, anaplastic astrocytoma, EGFR p.A289T, histone H3 wildtype

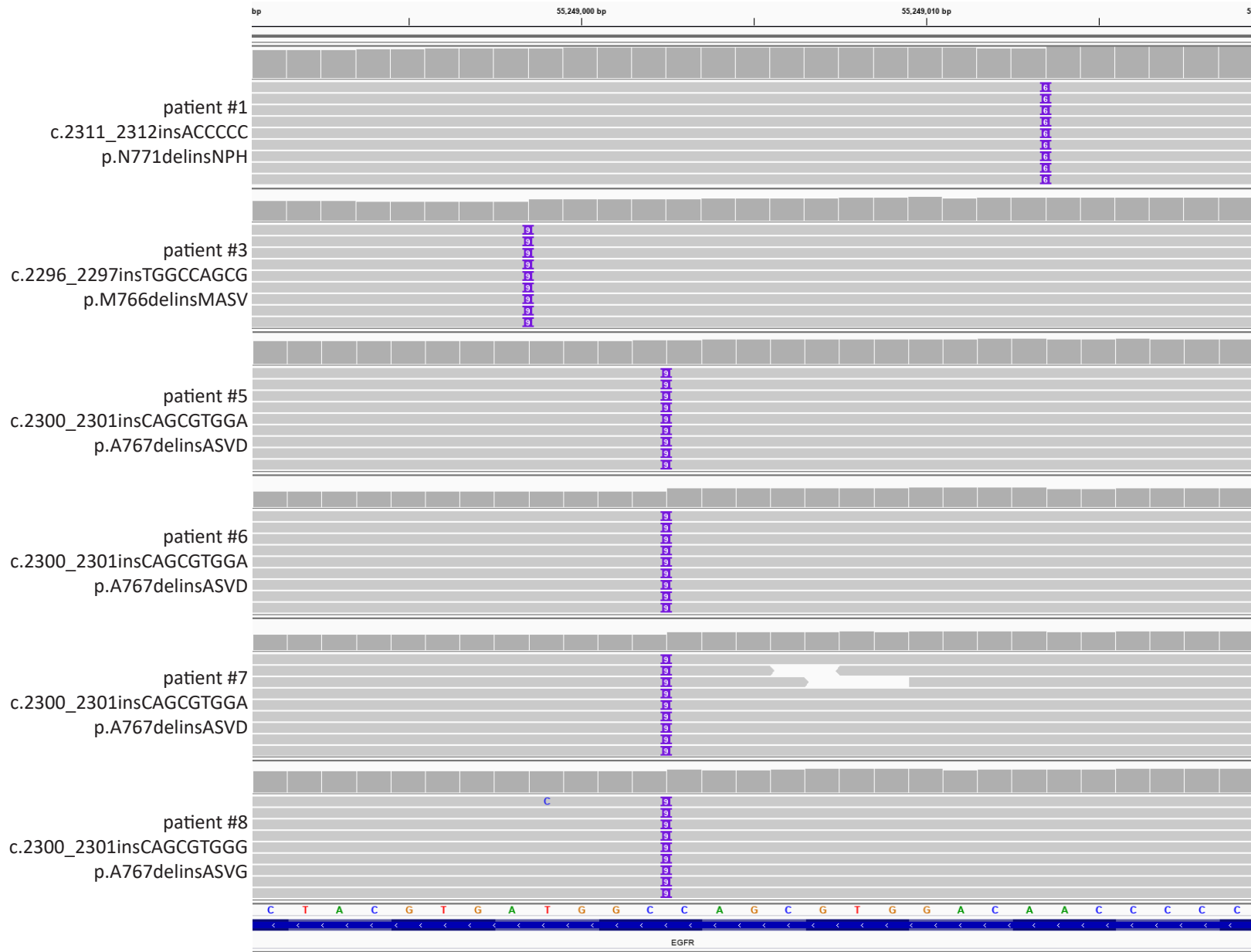


patient #11, 9 y/o girl, diffuse astrocytoma, EGFR p.A289V, HIST1H3B p.K27M



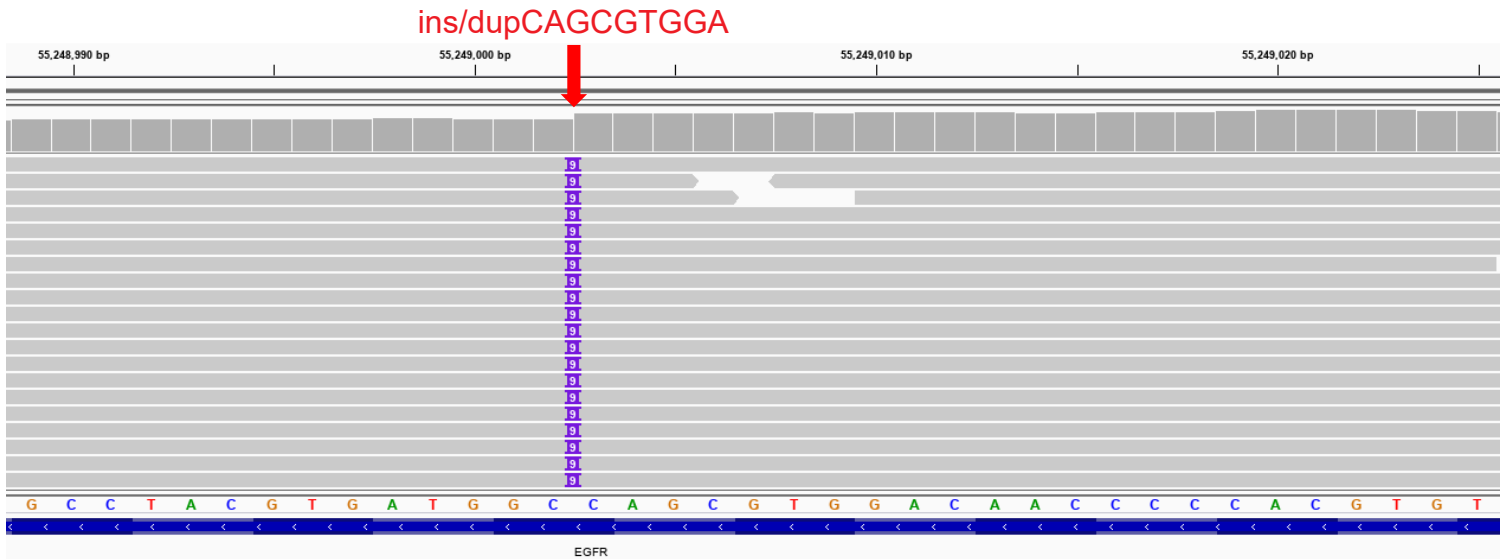
patient #13, 9 y/o boy, anaplastic astrocytoma, EGFR wildtype, histone H3 wildtype



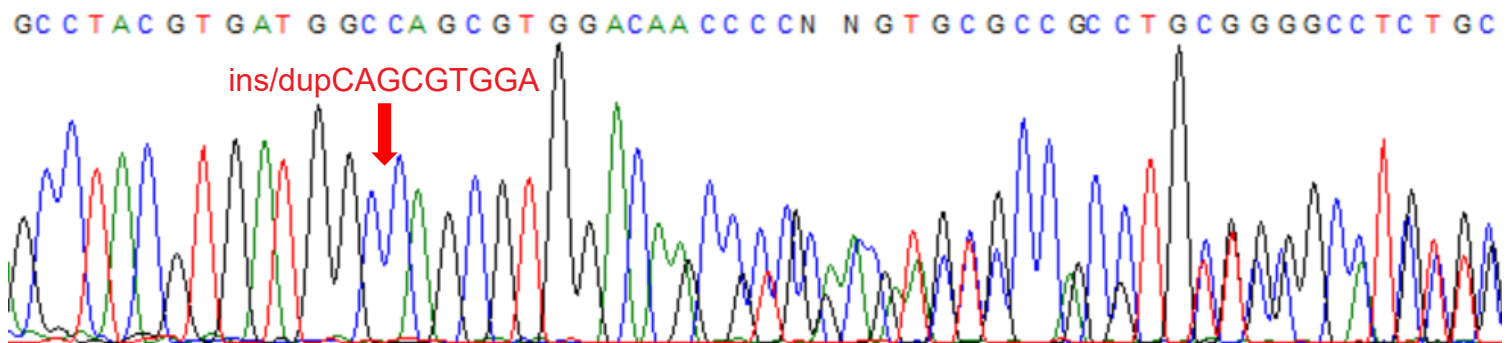


Supplementary Figure 3. Snapshots from the Integrated Genome Viewer of the *EGFR* exon 20 small in-frame insertion/duplications from six representative cases of pediatric bithalamic diffuse gliomas.

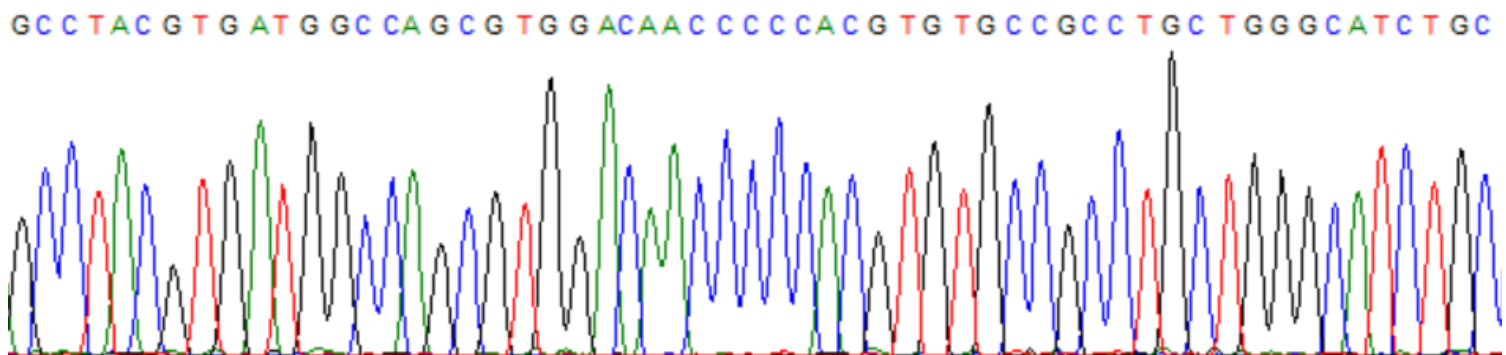
Bithalamic glioma from patient #7, *EGFR* exon 20 small in-frame insertion/duplication, p.A767delinsASVD



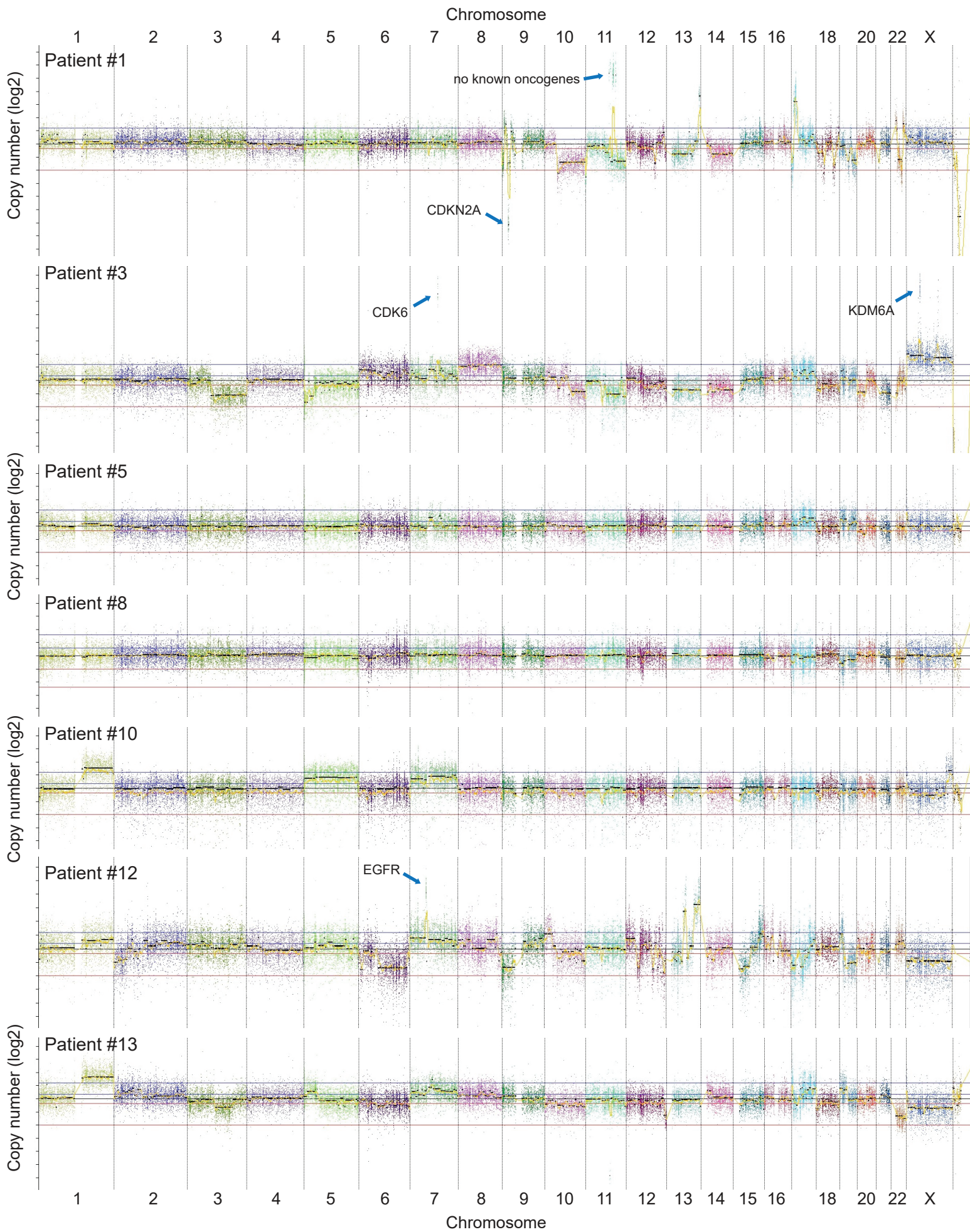
Bithalamic glioma from patient #7, *EGFR* exon 20 small in-frame insertion/duplication, p.A767delinsASVD



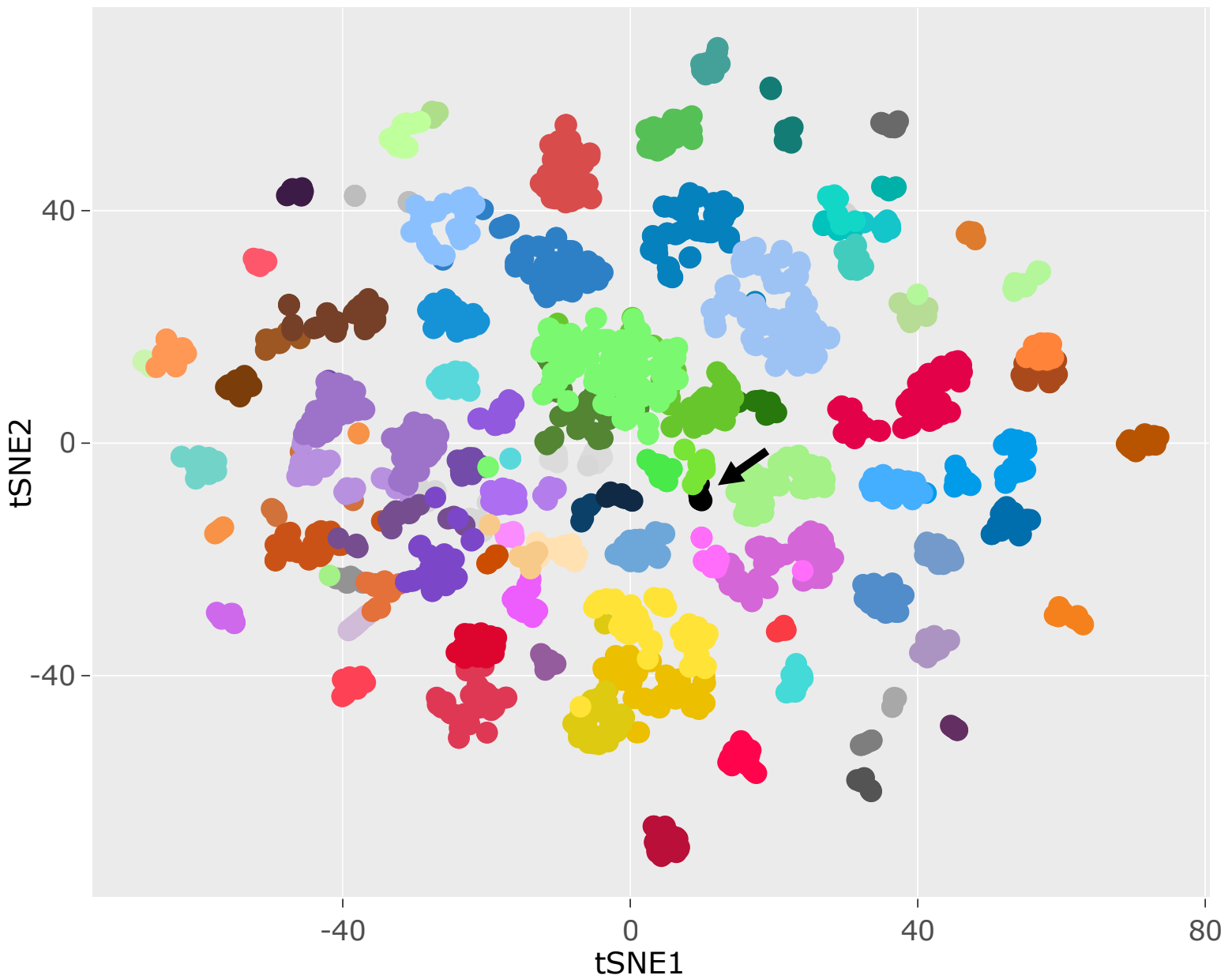
Medulloblastoma, *EGFR* exon 20 wildtype



Supplementary Figure 4. Sanger sequencing confirmation of the small in-frame insertion/duplication within exon 20 of the *EGFR* gene in the bithalamic glioma from patient #7. Snapshot from the Integrated Genome Viewer of the *EGFR* exon 20 small in-frame insertion/duplication based on the targeted next-generation sequencing data (top panel). Sanger sequencing trace for exon 20 of the *EGFR* gene following PCR amplification using genomic DNA from the bithalamic glioma from patient #7 or a medulloblastoma from an unrelated patient as template (bottom panel). The identical heterozygous small in-frame insertion/duplication of 9 nucleotides is observed in both the NGS data and the Sanger sequencing.

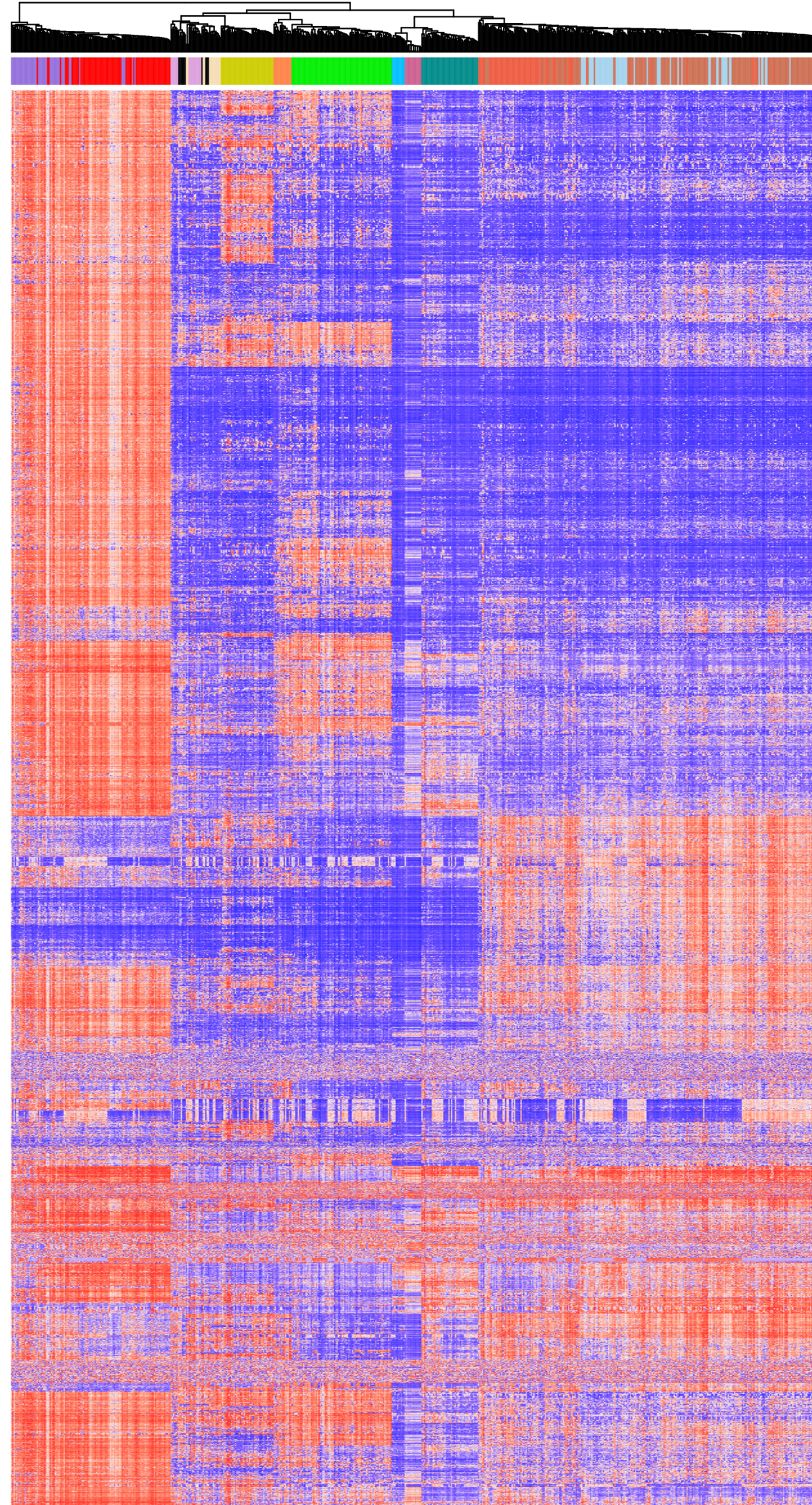


Supplementary Figure 6. Chromosomal copy number plots for representative pediatric bithalamic diffuse gliomas.



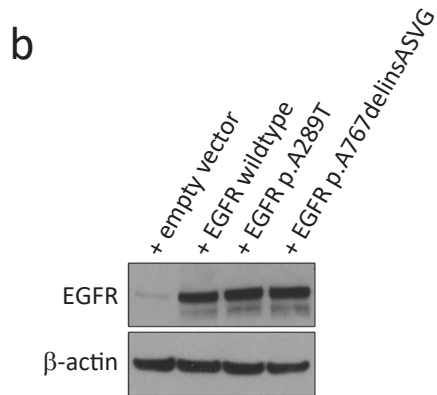
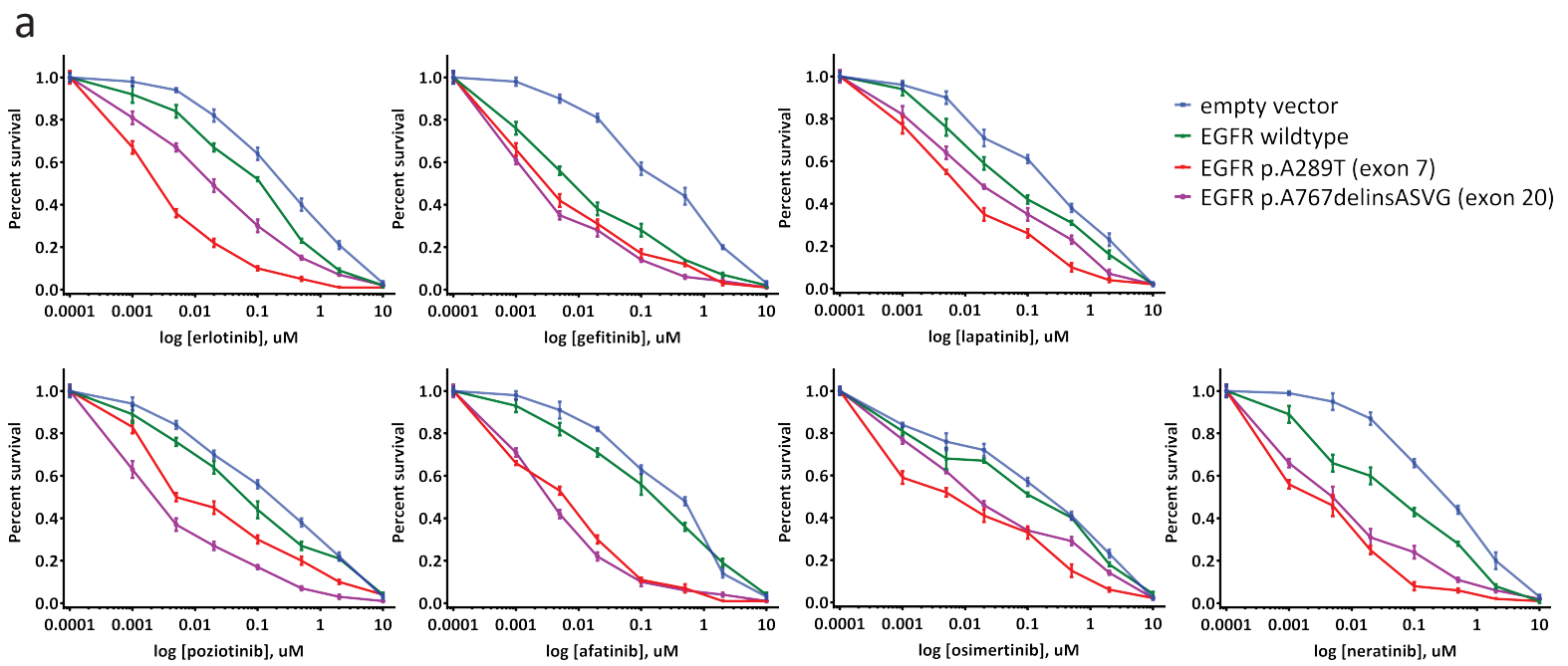
- | | | | | | | |
|-------------------|----------------|---------------|-----------------|-------------------|-----------------|----------------|
| ● A-IDH | ● CONTR-INFLAM | ● EPN-RELA | ● IHG | ● MB-SHH-INF | ● PITAD-STH-SPA | ● SUBEPN-SPINE |
| ● A-IDH-HG | ● CONTR-PINEAL | ● EPN-SPINE | ● LGG-DIG/DIA | ● MB-WNT | ● PITAD-TSH | ● SUBEPN-ST |
| ● ANA-PA | ● CONTR-PONS | ● EPN-YAP | ● LGG-DNT | ● MELAN | ● PITUI | |
| ● ATRT-MYC | ● CONTR-REACT | ● ETMR | ● LGG-GG | ● MELCYT | ● PLASMA | |
| ● ATRT-SHH | ● CONTR-WM | ● EWS | ● LGG-MYB | ● MNG | ● PLEX-AD | |
| ● ATRT-TYR | ● CPH-ADM | ● GBM-G34 | ● LGG-PA-MID | ● O-IDH | ● PLEX-PED-A | |
| ● BITHAL | ● CPH-PAP | ● GBM-MES | ● LGG-PA-PF | ● PGG-nC | ● PLEX-PED-B | |
| ● CHGL | ● DLGNT | ● GBM-MID | ● LGG-PA/GG-ST | ● PIN-T--PB-A | ● PTPR-A | |
| ● CHORDM | ● DMG-K27 | ● GBM-MYCN | ● LGG-RGNT | ● PIN-T--PB-B | ● PTPR-B | |
| ● CN | ● EFT-CIC | ● GBM-RTK-I | ● LGG-SEGA | ● PIN-T-PPT | ● PXA | |
| ● CNS-NB-FOXR2 | ● ENB-A | ● GBM-RTK-II | ● LIPN | ● PITAD-ACTH | ● RETB | |
| ● CONTR-ADENOPIIT | ● ENB-B | ● GBM-RTK-III | ● LYMPHO | ● PITAD-FSH-LH | ● SCHW | |
| ● CONTR-CEBM | ● EPN-MPE | ● HGNET-BCOR | ● MB-G3 | ● PITAD-PRL | ● SCHW-MEL | |
| ● CONTR-HEMI | ● EPN-PF-A | ● HGNET-MN1 | ● MB-G4 | ● PITAD-STH-DNS-A | ● SFT-HMPC | |
| ● CONTR-HYPHTHAL | ● EPN-PF-B | ● HMB | ● MB-SHH-CHL-AD | ● PITAD-STH-DNS-B | ● SUBEPN-PF | |

Supplementary Figure 7. tSNE plot of genome-wide methylation data from 10 pediatric bithalamic diffuse gliomas together with 2,801 reference samples spanning 82 CNS tumor entities and 9 control tissues.



Supplementary Figure 8.

Unsupervised hierarchical clustering of genome-wide DNA methylation data from 10 pediatric bithalamic gliomas together with 616 glioma reference samples from DKFZ using the 5,000 most differentially methylated CpG sites.



Supplementary Figure 9. a, Survival plots of immortalized human astrocytes (iNHAs) transduced with empty vector, EGFR wildtype, and EGFR mutant isoforms followed by treatment with various tyrosine kinase inhibitors at the indicated doses for 72 hours. Each data point is the mean of 6 replicates from two independent experiments, and error bars show standard error of the mean. **b**, Western blots on total cell lysate from immortalized human astrocytes (iNHAs) after lentiviral transduction with empty vector, EGFR wildtype, or EGFR mutant isoforms. An equal quantity of exogenous EGFR protein overexpression is seen with the wildtype and mutant isoforms.